Journal of Molecular Spectroscopy 397 (2023) 111836

Contents lists available at ScienceDirect

Journal of Molecular Spectroscopy

journal homepage: www.elsevier.com/locate/yjmsp

H_2O-HF dimer rotational spectra: New measurements and re-analysis

German Yu. Golubiatnikov [a], Oleg L. Polyansky [b,a], Nikolai F. Zobov [a], Jonathan Tennyson [b], Roman I. Ovsyannikov [a], Mikhail Yu. Tretyakov [a,*]

[a] Institute of Applied Physics, Russian Academy of Sciences, 46 Ulyanov Street, Nizhny Novgorod, 603950, Russia
[b] Department of Physics and Astronomy, University College London, Gower Street, London WC1E 6BT, United Kingdom

ARTICLE INFO

Keywords:
H_2O-HF dimer
Millimeter and sub-millimeter wave spectra
High resolution
Rotational constants

ABSTRACT

New measurements of the H_2O-HF dimer high resolution absorption spectrum are performed using a relatively warm (240–260 K) equilibrium gas mixture with two complementary spectrometers: a video spectrometer and spectrometer with radio-acoustic detection. Positions of over hundred H_2O-HF lines in the 158–345 GHz range are refined (their uncertainty is reduced by about order of magnitude) and several tens of lines are newly measured. These data are re-fitted together with previous measurements giving a refined set of constants of effective Hamiltonian which characterizes the dimer intermolecular dynamics. The new data improves significantly (from 100 to about 10 kHz) the accuracy of rotational constants corresponding to separate series of lines with fixed K_a.

1. Introduction

In this paper we initiate a return to a 30 years old problem stimulated by advances in both experiment and theory. The newly acquired ability to calculate accurately the spectra of floppy molecular complexes such as H_2O-HF on the basis of *ab initio* potential [1,2] prompted us to produce and assign improved experimental data for the purpose of comparison with and characterization of these calculations. In particular, we demonstrate a new possibility to resolve and measure components of the $K_a = 2$ and $K_a = 3$ doublets and assign lines belonging to the $K_a = 5$ branch. These branches had not been considered in our previous study [3], hereafter referred to as Paper I.

The study of weakly bound molecular complexes with hydrogen bonds and Van der Waals bonding accounts for a large sub-branch of molecular spectroscopy [4]. High resolution spectroscopy can provide very accurate information on these quantum systems but requires theoretical support to provide interpretation and understanding. The water dimer is key hydrogen-bonded, which plays important role in the Earth atmosphere [5–9] and is likely to also be important in the atmospheres of water-rich exoplanets [10]. Complete characterization of this dimer is the first crucial step in non-empirical physically based understanding of properties of liquid water, which is the basis of life on Earth.

Papers [11–13] demonstrate the possibility of observing the rotationally-resolved spectrum of the water dimer, and its partial characterization, at close to atmospheric conditions. These studies pave the way to a fuller understanding of the water dimer spectrum via a complete theoretical line list and further experimental observations (see, e.g., [14,15]). These important steps were made on the basis of unique complete rigorous quantum chemical calculations of the water dimer vibrational–rotational–tunneling spectrum in the range 0–750 cm^{-1} taking into account all vibrational states up to the hydrogen bond dissociation limit [16]. However, direct comparison of experimental water-dimer spectra with the results of modeling are not yet possible due to remaining imperfections in the calculations, including, in particular, inaccuracies introduced by the use of rigid-monomer approximation based potentials and the poorly-characterized highly-excited intermolecular vibrational states. These calculations could be improved with better experimental data, but this is unrealistic at present due to sensitivity (of the order of 10^{-15} cm^{-1} in terms of absorption coefficient) needed for any spectrometer to observe the high resolution spectrum of water dimer at temperatures where its vibrationally-excited states are sufficiently populated. Therefore, as discussed in [17], the only real benchmarking of the theoretical methods being used to compute the water dimer spectrum must be made via comparison of the calculations with experimental spectra of the two dimers iso-electronic to water dimer systems, namely HF-HF and H_2O-HF. The rotational lines of the H_2O-HF spectrum are sufficiently intense and its equilibrium constant is sufficiently large to allow observation of the high resolution spectrum at close to ambient temperatures with low-lying intramolecular vibrational modes of the dimer thermally populated.

The spectrum of H_2O-HF dimer was extensively studied experimentally, mostly in the microwave and sub-millimeter region, in the

* Corresponding author.
E-mail address: trt@ipfran.ru (M.Yu. Tretyakov).

https://doi.org/10.1016/j.jms.2023.111836
Received 29 June 2023; Received in revised form 22 August 2023; Accepted 16 September 2023
Available online 23 September 2023

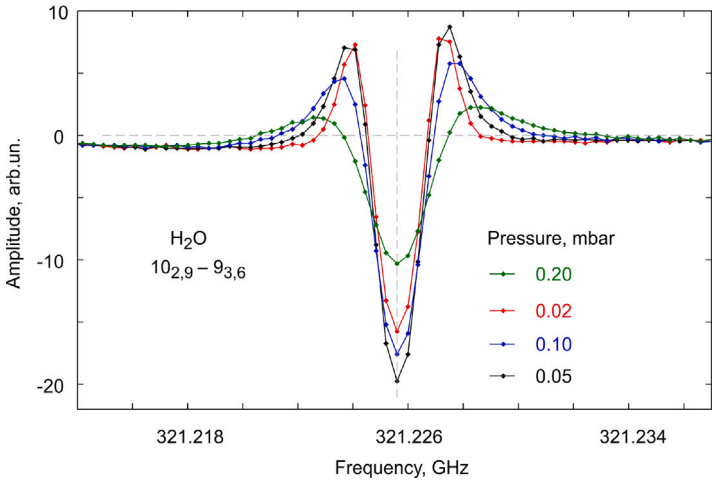

Fig. 1. Recordings of the 321-GHz water vapor line at several gas mixture pressures (see notations in the figure). Peak absorption in pure water vapor is 2.8×10^{-5} cm^{-1}. Tabulated position of the line and zero signal level are shown by dashed gray lines.

1980s [18–23]. Note that our aforementioned 2007 paper is based on work presented in older 1988 internal report of Institute of Applied Physics of the Russian Academy of Sciences [24]. The present paper is thus the first attempt to study the H_2O-HF rotational spectrum using modern experiment and theory.

The paper is organized as follows. The experimental setup is described in Section 2. Analysis of the recorded spectra, their comparison with the spectra from Paper I and results of the joint fit of all available high resolution data on the H_2O-HF spectrum is given in Section 3. Section 4 provides the conclusions and prospects for a future work.

2. Experimental details

The measurements of line positions were carried out using a backward-wave oscillator (BWO) based video spectrometer [25]. A two-pass stainless steel cell of length 70 cm and 11 cm diameter with high density polyethylene windows was used. The cell was wrapped in several layers of foamed polyethylene for thermal insulation. At the preparation stage recordings were made at room temperature but for the rest of the study the cell was pre-cooled to about 240–260 K prior the experiment by slowly pouring liquid nitrogen and kept cold during several hours. No automatic temperature regulation was used, so the thermodynamic conditions were not completely constant.

HF vapor was obtained by thermal decomposition of KFHF. The composition of the HF-H_2O gas mixture in the gas cell was regulated by adding water vapor from a separate flask. The water vapor content was monitored by observation of water lines near 183, 321 and 325 GHz (Fig. 1). The known intensity of these lines allows us to estimate the intensity of the H_2O-HF dimer lines. In most experiments the peak absorption was less than 10^{-6} cm^{-1} .

Typical working pressure was within 0.02–0.3 mbar (controlled by a baratron MKS 122 A gauge with a 10 mbar range). As a receiver of continuous-wave frequency-modulated radiation, a point contact detector with a planar Schottky diode was used, followed by demodulation by a synchronous amplifier at the second harmonic of the modulation frequency. The second harmonic method results in strong dependence of the signal magnitude on the line width. That is, if the frequency deviation (modulation index) is fixed, then as the pressure and the line width increases, the signal from the line decreases (Figs. 1, 3). An increase in the deviation leads to an increase of the baseline, which decreases the contrast of lines and the possibility of observing weak transitions. Strong baseline drift with temperature accompanied and complicated the observations.

The upper panel of Fig. 2 presents typical room temperature recordings of the spectrum in the vicinity of the quite intense H_2O-HF line

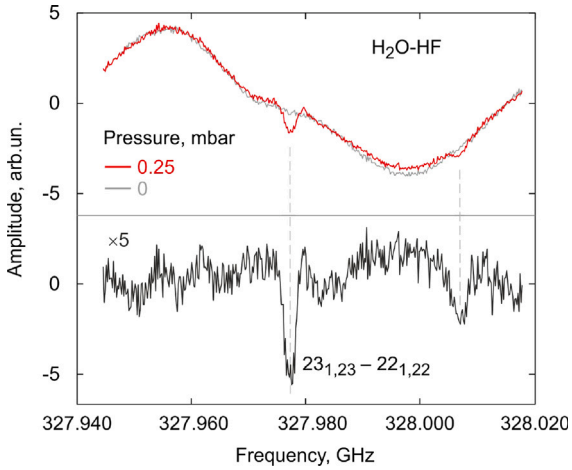

Fig. 2. Example of the H_2O-HF line $J_{Ka,Kc} = 23_{1,23} - 22_{1,22}$ at room temperature and total gas pressure of $p = 0.25$ mbar before (upper panel, red trace) and after (lower panel) the baseline (upper panel, gray trace) subtraction. Note 5× increased vertical scale in the lower panel and the unidentified H_2O-HF line near 328.007 GHz.

near 327.977 GHz with and without gas in the cell. The lower panel demonstrates improvement of the spectrum after the baseline subtraction. Fig. 3 presents recordings of the same part of the H_2O-HF spectrum at a number of pressures, corresponding to slow warming up the gas cell after its preliminary cooling.

The spectral resolution is much better than in previous measurements with RAD-3 spectrometer [3] because of the much lower pressures. For example, well-resolved doublets are observed for $K_a = 3$ transitions, see Fig. 4.

The very strong frequency dependence of the baseline and weak molecular absorption made broad-band recordings of the spectrum impossible. So measurements were made only in the vicinity of the line positions previously identified and reported in Paper I; rotational lines for the ground vibrational state (GS) transitions with J ranging from 11 to 24, up to $K_a = 4$, including several lines predicted as a continuation of previously observed series, were studied. Lines corresponding to excited vibrational states of the dimer were not measured except a few cases when they were in the vicinity of the measured GS lines. The HF-HF dimer lines reported previously [26,27] were not detected at our experimental conditions. Measurements were performed in the frequency range of 158–344 GHz covered by two BWOs of the type of OB-24 and OB-30. The moderate signal-to-noise ratio (SNR) and

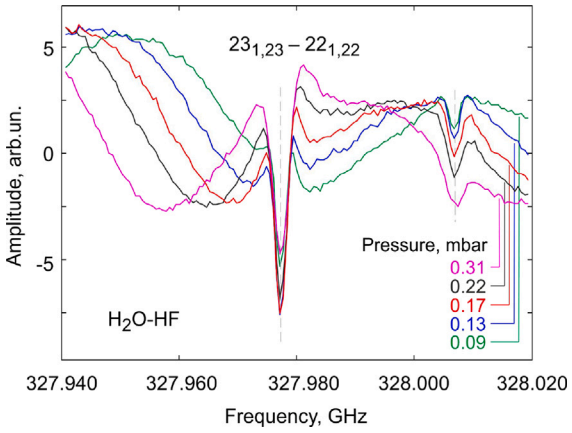

Fig. 3. Recordings of the same spectral interval as in Fig. 2 after pre-cooling the gas cell at several gas pressures (see notations in the figure).

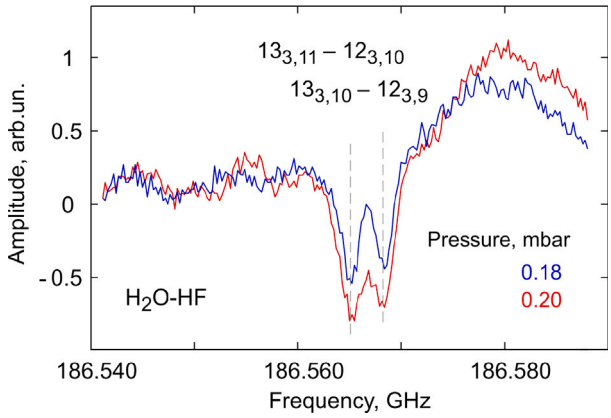

Fig. 4. Example of $K_a = 3$ doublet recordings near 186.567 GHz at two gas pressures.

significant impact of the spectrometer baseline limited the uncertainty of measurement of line centers to 100–200 kHz for well resolved lines.

Frequencies of all H_2O-HF dimer lines measured in this work are listed in Table 1 of the Supplementary material together with their assignments, positions from Paper I and residues from effective Hamiltonian fits to these data which were performed jointly with positions of pure rotational lines in the lowest intermolecular vibrational (out of plane bending) mode, hereafter denoted as ν_1, available from Paper I. Details of the fit are discussed in the next section.

Additional broad band recordings of the spectrum were made using the same phase-locked BWO-based radiation source and radio-acoustic gas cell similar to one used in Paper I. A typical example of such recordings are presented in Fig. 5 together with the corresponding spectrum from 1988 measured relatively reference SO_2 spectrum using RAD-3 spectrometer described in Paper I.

3. Data analysis

The uncertainty in the measured line positions of the 202 absorption lines of the ground and ν_1 state of the H_2O-HF molecule identified in Paper I was of the order of several MHz. These data were described using an effective Hamiltonian with 18 adjustable parameters and a simplified modeling of the Coriolis interaction between these two states, which was taken into account only for two rotational branches. The standard deviation of the fit residual was about 4 MHz. This accuracy was quite satisfactory, reflecting both the large experimental errors and the very approximate way of treating the Coriolis interaction. In the present work we consider this accuracy as the reference one.

The program SPFIT [28–30] (available from http://spec.jpl.nasa.gov/) was used for the analysis. Following [31], we employed a coupled two-state Hamiltonian $\hat{H} = \begin{pmatrix} \hat{H}_{00} & \hat{P}_{cor} \\ -\hat{P}_{cor} & \hat{H}_{11} + E \end{pmatrix}$, where $\hat{H}_{00}$ and $\hat{H}_{11}$ are the A-reduced semirigid rotor Hamiltonians for the ground and ν_1 state, respectively, with coefficients expanded up to the sextic distortion terms (which is similar to the Hamiltonian used in Paper I); E is the vibrational energy of the ν_1 state and $\hat{P}_{cor}$ is the Coriolis interaction term. The Coriolis interaction is represented as a power series of $\hat{P} = \hat{J}_a\hat{J}_c + \hat{J}_c\hat{J}_a$ operator: $\hat{P}_{cor} = F_{ca.J}\hat{P}\hat{J} + F_{ca.K}\hat{P}\hat{J}_z + F_{ca.JJ}\hat{P}\hat{J}\hat{J} + F_{ca.JK}\hat{P}\hat{J}\hat{J}_z + F_{ca.KK}\hat{P}\hat{J}_z\hat{J}_z$. The total number of adjustable parameters is 28.

The initial dataset from Paper I was used in the first step of the analysis as is. Lines adopted from [23] were assumed to have uncertainties of 0.3 MHz for $K_a \leq 1$ and 1 MHz for $K_a > 1$. An uncertainty of 2 MHz was assumed for all other lines. The initial value of the E parameter was taken from Ref. [19]. The main problem of fitting the Hamiltonian to this dataset turned out to be the difficulty in determining the values of the rotational constants A. If unrestricted, these parameters may take negative or unreasonably large values. To resolve the problem, the initial values of the A constants were set close to the values used in Paper I, and the step for calculating the energy derivatives with respect to this parameter was set to 10 MHz, much smaller than the values of the constant (about 100 GHz). After these modifications the initial dataset was reproduced by the fitted Hamiltonian with a standard deviation of 2.4 MHz. The fit coefficients of the Hamiltonian obtained are presented in column I of Table 1. The improved fit quality compared to Paper I is the result of properly taking into account the Coriolis interaction, the larger number of adjustable parameters in the Hamiltonian and use of appropriate experimental uncertainties.

As the next step in the analysis we updated the frequencies for lines with J ranging from 12 to 24 and K_a from 0 to 4, which were remeasured in this work, including 94 GS lines and 6 lines in the ν_1 state. Compared to [3], the higher spectral resolution (lower pressure) and higher measurement accuracy (measurements with a frequency synthesizer rather than the reference spectrum) made it possible to observe a previously unresolved splitting of 6 lines of the $K_a = 2$ branch and 12 lines of the $K_a = 3$ branch in the GS. A frequency uncertainty of 0.2 MHz was assumed for all newly measured lines in the fitting procedure.

However, the small frequency uncertainty of the 82 lines replaced by new measurements and the 18 additional lines the from newly resolved doublets made the fit unstable. The lines retained from Paper I with a 2-MHz assumed uncertainty deviated from their predicted positions by up to tens of MHz. To stabilize the fit and to find a good set of initial parameters, we made an intermediate fit with 1-MHz uncertainty for all lines. After that the standard deviation of the fit from the dataset (with normal uncertainties restored) decreased to 1.94 MHz. Spectroscopic constants obtained at this step are listed in column II of Table 1.

These constants were used to predict and confidently identify 11 lines of H_2O-HF dimer with $J = 11 \leftarrow 10$ and $12 \leftarrow 11$ in the observed spectrum, extending the already known branches with K_a from 0 to 3 into the 155–175 GHz range, which were not sampled previously. These lines were added to our final dataset (Table 1 in the Supplementary material).

An additional attempt was made to detect the $K_a = 5$ branch in the GS of the dimer. Positions of these lines were predicted using the same set of effective constants. Three lines in the observed spectrum were found in a good agreement with the predicted pattern and added to the final dataset. Spectroscopic parameters obtained from fitting the Hamiltonian to the final dataset are collected in column III of Table 1. The overall dataset is reproduced by these constants with a standard deviation 1.9 MHz. Note that most of the line frequencies in the ν_1 state (forming near one half of the final dataset) were used in the fit here and their estimated uncertainty is several MHz. This explains the

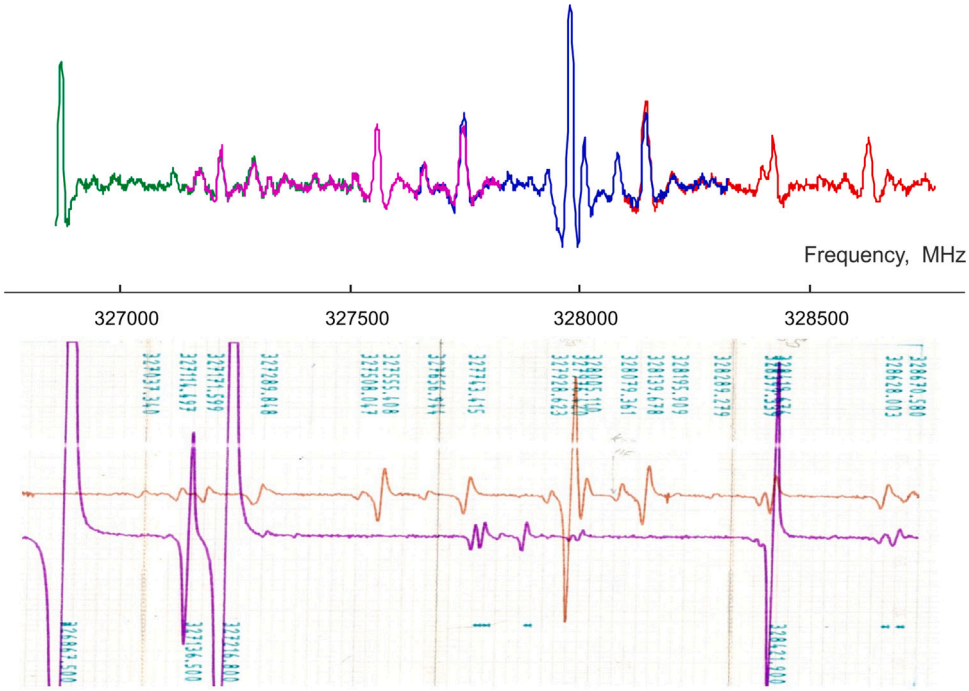

Fig. 5. New broad-band recordings of the H_2O-HF spectrum with radio-acoustic gas cell and frequency synthesizer (upper panel) in comparison with a recording from Paper I (lower panel, upper trace). Different colors in the upper panel correspond to consequential recordings with different ways of frequency synthesis. Overlapping parts of the traces demonstrate repeatability between different scans.

Table 1
Fitted Hamiltonian constants for H_2O-HF rotational lines in the ground (upper half of the table) and ν_1 vibrational state (lower half of the table) for three datasets. Our final constants are given in column III (see text for details).

	Constant	Units	I	II	III
GS	A	GHz	505.0651(100)	505.0635(100)	505.0619(100)
	B	MHz	7388.51(43)	7388.605(81)	7388.623(80)
	C	MHz	7014.39(43)	7014.130(81)	7014.143(81)
	$-D_J$	kHz	−36.762(41)	−36.4813(155)	−36.5143(134)
	$-D_{JK}$	MHz	−1.8726(57)	−1.88308(152)	−1.88566(135)
	$-D_K$	MHz	−70.0(52)	−68.80(137)	−69.02(120)
	$-d_J$	kHz	−0.4893(148)	−0.4686(50)	−0.4702(46)
	$-d_K$	MHz	−62.598(215)	−62.695(40)	−62.694(40)
	H_J	Hz	−0.301(39)	−0.5446(129)	−0.5215(115)
	H_{JK}	kHz	11.928(81)	11.9756(152)	11.9771(151)
	H_{KJ}	kHz	−25.35(41)	−25.195(104)	−25.144(93)
ν_1	E	GHz	1901.666(859)	1876.354(969)	1903.965(803)
	A	GHz	553.2871(100)	553.2877(100)	553.2879(100)
	B	MHz	7413.29(99)	7414.82(40)	7414.80(38)
	C	MHz	7103.97(99)	7102.43(40)	7102.45(38)
	$-D_J$	kHz	−36.661(65)	−36.357(47)	−36.355(47)
	$-D_{JK}$	MHz	−2.0795(112)	−2.0885(97)	−2.0900(96)
	$-D_K$	MHz	−708.5(93)	−677.1(89)	−674.5(51)
	$-d_J$	kHz	−0.5598(210)	−0.5338(164)	−0.5307(162)
	$-d_K$	MHz	−53.27(49)	−54.067(197)	−54.059(188)
	H_J	Hz	−0.460(72)	−0.768(47)	−0.765(47)
	H_{JK}	kHz	8.005(149)	8.213(60)	8.210(58)
	H_{KJ}	kHz	75.73(89)	75.70(68)	76.00(62)
Coriolis	$F_{ca.J}$	kHz	72.9(48)	77.10(228)	74.33(179)
	$F_{ca.K}$	MHz	65.4786(100)	65.4810(100)	65.4838(100)
	$F_{ca.JJ}$	Hz	−42.4(52)	−59.51(135)	−58.90(130)
	$F_{ca.JK}$	kHz	−3.65(61)	−3.48(49)	−3.26(36)
	$F_{ca.KK}$	kHz	−493.26(100)	493.47(100)	493.42(100)

relatively small improvement of the fit quality compared to 2.4 MHz given by the initial dataset. Note that our step-by-step improvement of the dataset has led to the refinement of effective constants. The uncertainty of rotational and centrifugal constants of the GS is reduced by factor of 3 – 4 and the change of these constants is within estimated uncertainties (see Table 1). However, the deviation between observed and calculated GS line positions in most cases significantly exceeds the experimental uncertainty (standard deviation for all GS lines is 0.74 MHz). This deviation may be an indication that the Hamiltonian is not quite appropriate for describing strongly interacting states in such a non-rigid molecule.

To resolve the problem of accurate analysis of experimental data we used a simple equation for transition frequencies of a diatomic

Table 2
B_e, D_e, and H_e parameters (in MHz), determined from the fit by Eq. (1) for separate series of GS lines with the same K_a. Plus and minus signs are used for notation of the upper and lower frequency component of the doublet.

K_a	B_e	D_e	H_e
0	7201.507(10)	0.037842(30)	−3.18(27)e-07
1+	7168.627(11)	0.036320(34)	−3.04(30)e-07
1−	7230.514(10)	0.037384(29)	−3.73(27)e-07
2+	7193.920(17)	0.036502(49)	−2.43(44)e-07
2−	7193.886(14)	0.035333(40)	−3.66(36)e-07
3+	7187.644(14)	0.035554(42)	−5.83(38)e-07
3−	7187.710(28)	0.035383(84)	−7.18(76)e-07
4	7177.583(17)	0.035631(47)	−3.75(40)e-07

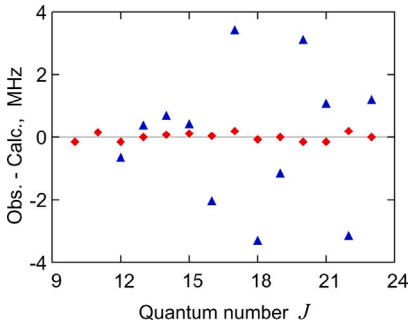

Fig. 6. Deviation of measured line frequencies of $K_a = 0$ series from fitted diatomic spectrum (Eq. (1)) for data from Paper I (blue triangles) and from this work (red diamonds).

molecule:

$$\nu(J) = 2B_e(J+1) - 4D_e(J+1)^3 + H_e(J+1)^3((J+2)^3 - J^3) \quad (1)$$

where J is the lower level rotational quantum number of the transition and B_e, D_e, H_e are effective constants. The equation was fitted to our newly measured line frequencies of the $K_a = 0$, 1, 2, 3 and 4 series. Residuals of the fit and values of corresponding constants are reported in Dev. II column of Table 1 in the Supplementary material and in Table 2, respectively. Standard deviation of these series-by-series analysis residuals is 0.26 MHz, which is in agreement with the estimated experimental uncertainties.

To demonstrate the our increased measurement accuracy the fit was repeated for the $K_a = 0$ series using data from Paper I. The results obtained are given in Fig. 6. Standard deviation of the data from the fitted Eq. (1) are 0.125 and 2.1 MHz for this work and for Paper I, respectively. Rotational constants B_e obtained from these fits: 7201.508(10) and 7201.529(96) MHz for the new and old data, respectively, coincide with each other within uncertainty limits (note order of magnitude reduction of the uncertainty) and deviate by less than 0.15 MHz from the value of $(B + C)/2 = 7201.383(114)$ MHz obtained using the results of the total fitting (Table 1).

A few more lines of the dimer corresponding to the $J = 27 \leftarrow 26$ transition with different K_a were measured using the RAD spectrometer with an accuracy of about 1 MHz after the initial work was completed. We decided to use these data to verify the line position predictions by the spectroscopic constants obtained in this work. The measured frequencies are listed in Table 3 together with their deviations from the calculated values using the final set of constants from Table 1 and the B_e, D_e and H_e constants from Table 2. This trial demonstrates an advantage of the series-by-series analysis of the dimer spectrum and confirms the conclusion that the constants from Table 1 should be considered as effective ones.

Note that the energy of the ν_1 state determined from the fit in this work (Table 1, $E = 1903.965(803)$ MHz = 63.51(3) cm^{-1}) is in a good agreement with 64(10) cm^{-1} determined by Kisiel [19] on the basis of line relative intensities analysis but about 20 cm^{-1} smaller than the

Table 3
Measured line frequencies (column I) used for verification of the spectral predictions. Columns II and III are the prediction uncertainty and obs.-calc. for the final set of constants from Table 1, and columns IV and V are the same for the fixed K_a series prediction using B_e, D_e and H_e constants. All values are in MHz.

Transition	I	II	III	IV	V
$27_{0,27} - 26_{0,26}$	385 873.5	0.2	0.7	0.6	−1.1
$27_{1,27} - 26_{1,26}$	384 220.4	0.3	3.8	0.6	0.3
$27_{1,26} - 26_{1,25}$	387 473.2	0.3	6.7	0.6	0.9
$27_{2,26} - 26_{2,25}$	385 575.2	0.3	−5.0	0.9	−1.7
$27_{2,25} - 26_{2,24}$	385 657.4	0.3	−5.3	0.7	0.9
$27_{3,25} - 26_{3,24}$	385 289.8	0.3	−11.9	0.8	1.1
$27_{4,24} - 26_{4,23}$	384 752.2	0.3	−10.8	0.7	0.3

values obtained from Refs. [1,2] from *ab initio* calculations. The discrepancy between theory and our empirical fit exceeds the fit uncertainty in about three orders of magnitude; in our opinion this is not the reflection of inaccuracy of *ab initio* calculations but an additional indication of the effective character of the constants obtained from the fit.

Figure 7 and its extended version given in the Supplementary material present a review of the H_2O-HF spectrum in the range studied. Only broad-band spectra recorded by the RAD-3 spectrometer in 1988 are shown. Gaps in the spectrum appear partly because of loss of the initial digital recording data and partly because uninformative (as we believed in 1988) spectral intervals were skipped. These recordings were recovered from legacy paper spectra using RECSPE software package developed by Z. Kisiel [32] (available from http://info.ifpan.edu.pl/~kisiel/prospe.htm). All recordings are centered at the frequency of the $K_a = 0$ GS transitions. Only series identified in Paper I are marked. Many other series, which are clearly seen in the figures remain unassigned. The accuracy of the line positions in Paper I was one of the reasons why only the ν_1 state lines were assigned out of lines from many other vibrational states. We demonstrate now that it is possible to determine line positions with uncertainty of 100–200 kHz which should allow the assignment of lines in higher excited states using information on their rotational constants. This information can be obtained from spectral simulation on the basis of quantum dynamical calculation of nuclear motions using an *ab initio* potential energy surface (such spectra hereafter will be called *ab initio* spectra) as explained below.

A comparison of B constants determined in this work on the basis of experimental spectra (Table 1) with values reported in Table 9 of Ref. [1] obtained from *ab initio* spectrum shows that the discrepancy between observed and calculated values is 120–150 MHz. For reliable identification of new features, the accuracy of such "*ab initio* constants" needs to be significantly higher than achieved in Ref. [1]. As a demonstration of capability of theoretical methods to achieve such a high accuracy we cite Ref. [17] where the discrepancy between the experimental and *ab initio* B_e constants of $(HF)_2$ dimer for the excited K_a of the GS is between 2 and 6 MHz, comparable with the experimental accuracy which was also several MHz. This gives hope that significantly better accuracy for the effective rotational B_e-constants for the H_2O-HF dimer could be obtained using a higher level of *ab initio* theory, namely, the higher dimensionality of the potential energy surface, extension of the basis set, increasing the correlation and, including adiabatic, relativistic corrections and other improvements such as those used in Ref. [17].

3.1. J-branches in the excited vibrational states

The A constants of the H_2O-HF dimer are estimated to be in the region of 13 cm^{-1}. The energy of K_a states can be estimated as AK_a^2 suggesting that the $K_a = 4$ states of the GS should lie about 210 cm^{-1} above the zero point energy. Note that corresponding transitions were measured for both the ground and ν_1 states for practically all J values considered in this work (see Fig. 7). In order to estimate the SNR of the $K_a = 0$ and $K_a = 1$ rotational lines, belonging to an excited vibrational

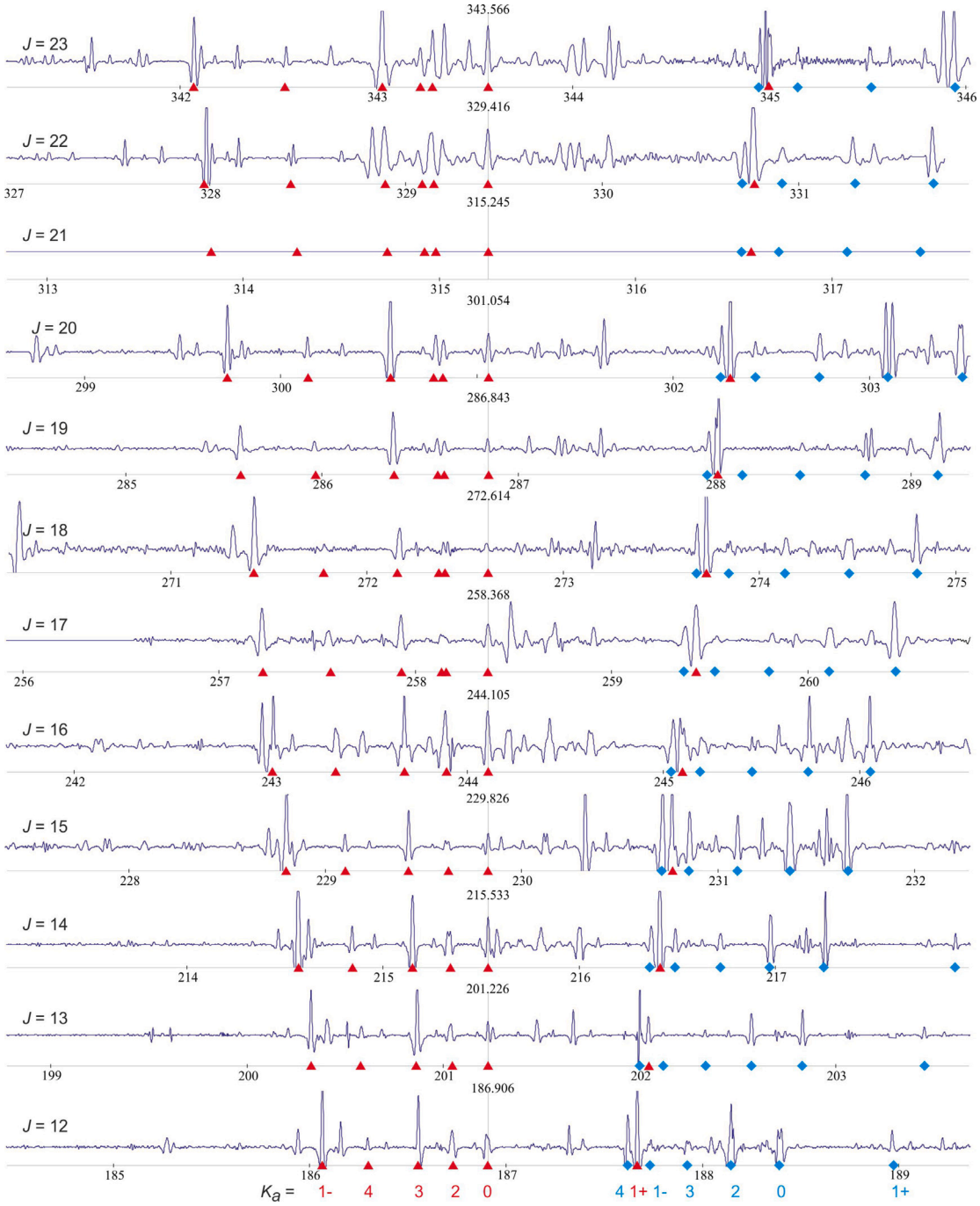

Fig. 7. Recordings of H_2O-HF spectrum obtained using RAD-3 [3] and centered at the frequency of $K_a = 0$, GS transition. Identified series are marked by red triangles and blue diamonds for the GS and ν_1 state, respectively.

state, we need to estimate the Boltzmann factor by which the intensities of its pure rotational lines in the millimeter and submillimeter-wave range decrease in comparison with $K_a = 0$ lines of the GS. These factors at temperature of 259 K, corresponding to the mean conditions of our experiments, are given in Table 4 alongside a list of excited vibrational states of potential interest, the values of the vibrational energies as estimated by Thomas [33] from early empirical information, the corresponding values estimated from analysis of experimental lines intensities [18–22] and from *ab initio* calculations [1]. One can see that $K_a = 0$ and $K_a = 1$ lines for vibrational states located below 300 cm^{-1} are only about five times weaker than the corresponding GS lines and, therefore, can be observed with the sufficient SNR. Indeed, the rotational spectrum of six vibrational states should be observable using our setup and their B_e values could be determinable for comparison with the future accurate *ab initio* spectra. Furthermore, measurements of the relative line intensity will give us additional information for reliable identification of series of lines in various excited vibrational states. There are other influences on the intensity ratios besides the Boltzmann factor which can be also taken into account using modern theoretical methods as in Ref. [16]. That will give us further information on the characterization of the accuracy of H_2O-HF *ab initio* calculations in the future. All these studies will be the subject of the future work.

Table 4
Lowest rotational and vibrational levels of the H_2O-HF dimer in cm^{-1} .

Band[a]	Ref. [33]	Ref. [19]	Ref. [1]	BF[b]
$GS, \quad K_a = 0$	0	0	0[d]	1.0
$K_a = 1$			13[d]	0.93
$K_a = 2$			52[d]	0.74
$K_a = 3$			117[d]	0.51
$K_a = 4$			208[d]	0.30
$K_a = 5$			325[d]	0.15
$K_a = 6$			468[d]	0.07
$\nu_{\beta(o)}$[c]	145(50)	64(10)	81.862	0.62
$\nu_{\beta(i)}$	170(50)	157(10)	196.131	0.32
ν_σ	180(30)	176(15)	195.997	0.32
$2\nu_{\beta(o)}$		228(15)	238.228	0.25
$\nu_\sigma + \nu_{\beta(o)}$			281.782	0.20
$\nu_{\beta(o)} + \nu_{\beta(i)}$		267(35)	299.073	0.18
$2\nu_\sigma$			381.931	0.11
$2\nu_{\beta(i)}$			385.970	0.11
$\nu_\sigma + \nu_{\beta(i)}$			389.844	0.11
$3\nu_{\beta(o)}$			394.781	0.10
$\nu_\sigma + 2\nu_{\beta(0)}$			436.626	0.08
$2\nu_{\beta(o)} + \nu_{\beta(i)}$			459.312	0.07
$2\nu_\sigma + \nu_{\beta(o)}$			470.856	0.07
$\nu_{\beta(o)} + \nu_\sigma + \nu_{\beta(i)}$			495.276	0.06
$\nu_{\beta(o)} + 2\nu_{\beta(i)}$			511.467	0.05
$3\nu_\sigma$			558.902	0.04
$4\nu_{\beta(o)}$			563.212	0.04
$3\nu_{\beta(i)}$			566.501	0.04
$2\nu_\sigma + \nu_{\beta(i)}$			574.142	0.04
$\nu_\sigma + 2\nu_{\beta(i)}$			575.441	0.04
$\nu_{B(o)}$	666(30)		577.164	0.04
$\nu_{B(i)}$	696(30)		679.791	0.02

[a] Vibrational band notation in accordance with Ref. [20].
[b] Boltzmann factors at 250 K calculated using vibrational energies from Ref. [1].
[c] Denoted as ν_1 in this work and in Paper I.
[d] Derived from the formula $E = AK_a^2$ with the A constant taken from Ref. [1].

4. Conclusion

The HF dimer and the HF-H_2O dimer are the two systems which represent the closest analogs to the water dimer from two different perspectives. The HF dimer mimics the water dimer tunneling spectra the best and H_2O-HF dimer is the closest from the viewpoint of vibrations and rotational B constants. The overwhelming advantage of these two dimers over the water dimer from the viewpoint of understanding the accuracy of *ab initio* theory is that it is possible to record their high resolution spectra for many ro-vibrational states at equilibrium close to atmospheric conditions. Thus the study of the rovibrational spectra of these two dimers opens the way to characterize the accuracy of *ab initio* calculations for the water dimer. HF dimer has been much better studied with many papers analyzing its IR spectra due mostly to Quack and Suhm (see references in their paper [34] and related references in [17]).

The spectrum of H_2O-HF dimer awaits more thorough study. This dimer does not display inversion-tunneling motion like the water- and HF-dimers, and, as a result, observation of high J lines in excited vibrational states is possible in the submillimeter-wave region. An accurate measurements of the relative intensities of pure rotational lines belonging to different vibrational states of the dimer will provide additional information to aid the reliable identification of these lines. Thus extensive experimental information on different vibrational states can be obtained using the millimeter-submillimeter wave region. With the present paper we restart this important process, which faded away about 15 years ago. The lines with the K_a up to 4 in the GS are remeasured with high accuracy and the $K_a = 5$ series is tentatively identified for the first time. The SNR of the newly observed lines and significantly improved spectral resolution demonstrate our ability to observe rotational lines in at least six low lying excited vibrational states and to provide important information for comparison with *ab initio* spectra contributing to a deep understanding of the complex intermolecular dynamic of dimers.

Declaration of competing interest

The authors declare that they have no known competing financial interests or personal relationships that could have appeared to influence the work reported in this paper.

Data availability

The data are submitted together with the article as supplementary material.

Acknowledgments

The experiments were carried out using the Large-scale research facilities “CKP-7” (USU No. 3589084). We express our gratitude to Anastasiya Sekacheva for digitizing the legacy paper spectra of H_2O-HF from 1988. We also thank the UK Natural Environment Research Council (NERC) grant NE/T000767/1 and ERC Advanced Investigator Project 883830 for supporting theoretical aspects of this project. RF State Project 0030-2021-0016 is also acknowledged.

Appendix A. Supplementary data

Supplementary material related to this article can be found online at https://doi.org/10.1016/j.jms.2023.111836. The material includes: (i) the list of lines measured in this work together with their assignments, positions from Paper I and residues from effective Hamiltonian fits to these data, (ii) Extended analog of Fig. 7, and (iii) SPFIT input and output files for the global fit of all known identified lines.

References

[1] D. Viglaska, X.-G. Wang, T. Carrington Jr., D.P. Tew, Computational study of the rovibrational spectrum of H_2O-HF, J. Mol. Spectrosc. 384 (2022) 111587, http://dx.doi.org/10.1016/j.jms.2022.111587.

[2] J. Loreau, Y.N. Kalugina, A. Faure, A. van der Avoird, F. Lique, Potential energy surface and bound states of the H_2O...HF complex, J. Chem. Phys. 153 (2020) 214301, http://dx.doi.org/10.1063/5.0030064.

[3] S.P. Belov, V.M. Demkin, N.F. Zobov, E.N. Karyakin, A.F. Krupnov, I.N. Kozin, O.L. Polyansky, Tretyakov M.Yu., Microwave study of the submillimeter spectrum of the H_2O...HF dimer, J. Mol. Spectrosc. 241 (2007) 124–135, http://dx.doi.org/10.1016/j.jms.2006.11.008.

[4] D.J. Nesbitt, High-resolution infrared spectroscopy of weakly bound molecular complexes, Chem. Rev. 88 (6) (1988) 843–870.

[5] P. Chylek, D.J. Geldart, Water vapor dimers and atmospheric absorption of electromagnetic radiation, Geophys. Res. Lett. 24 (1997) 2015—2018.

[6] J.S. Daniel, S. Solomon, H.G. Kjaergaard, D.P. Schofield, Atmospheric water vapor complexes and the continuum, Geophys. Res. Lett. 31 (2004) L06118.

[7] G.K. Schenter, S.M. Kathmann, B.C. Garett, Dynamical nucleation theory: a new molecular approach to vapor-liquid nucleation, Phys. Rev. Lett. 82 (1999) 3484–3487.

[8] K.P. Shine, I.V. Ptashnik, G. Rädel, The water vapour continuum: brief history and recent developments, Surv. Geophys. 33 (3–4) (2012) 535–555.

[9] V. Vaida, Perspective: Water cluster mediated atmospheric chemistry, J. Chem. Phys. 135 (2011) 020901.

[10] L. Anisman, K.L. Chubb, J. Elsey, A. Al-Refaie, Q. Changeat, S.N. Yurchenko, J. Tennyson, G. Tinetti, Cross-sections for heavy atmospheres: H_2O continuum, J. Quant. Spectrosc. Radiat. Transfer 278 (2022) 108013, http://dx.doi.org/10.1016/j.jqsrt.2021.108013.

[11] Tretyakov, M.Yu., E.A. Serov, M.A. Koshelev, V.V. Parshin, A.F. Krupnov, Water dimer rotationally resolved millimeter-wave spectrum observation at room temperature, Phys. Rev. Lett. 110 (9) (2013) 093001, http://dx.doi.org/10.1103/PhysRevLett.110.093001.

[12] E.A. Serov, M.A. Koshelev, T.A. Odintsova, V.V. Parshin, Tretyakov, M.Yu., Rotationally resolved water dimer spectra in atmospheric air and pure water vapour in the 188–258 GHz range, Phys. Chem. Chem. Phys. 16 (47) (2014) 26221–26233.

[13] M.A. Koshelev, I.I. Leonov, E.A. Serov, A.I. Chernova, A.A. Balashov, G.M. Bubnov, A.F. Andriyanov, A.P. Shkaev, V.V. Parshin, A.F. Krupnov, Tretyakov, M.Yu., New frontiers in modern resonator spectroscopy, IEEE Trans. Terah. Sci. Techn. 8 (6) (2018) 773–783.

[14] T.A. Odintsova, Tretyakov, M.Yu., A.O. Zibarova, O. Pirali, P. Roy, A. Campargue, Far-infrared self-continuum absorption of $H_2^{16}O$ and $H_2^{18}O$ (15 500 cm^{-1}), J. Quant. Spectrosc. Radiat. Transfer 227 (2019) 190–200.

[15] T.A. Odintsova, Tretyakov, M.Yu., A.A. Simonova, I.V. Ptashnik, O. Pirali, A. Campargue, Measurement and temperature dependence of the water vapor self-continuum between 70 and 700 cm^{-1}, J. Mol. Struct. (2020) 128046.

[16] Y. Scribano, C. Leforestier, Contribution of water dimer absorption to the millimeter and far infrared atmospheric water continuum, J. Chem. Phys. 126 (2007) 234301, http://dx.doi.org/10.1063/1.2746038.

[17] R.I. Ovsyannikov, V.Y. Makhnev, N.F. Zobov, J. Koput, J. Tennyson, O.L. Polyansky, Highly accurate HF dimer *ab initio* initio potential energy surface, J. Chem. Phys. 156 (2022) 164305, http://dx.doi.org/10.1063/5.0083563.

[18] J. Bevan, A. Legon, D. Millen, S. Rogers, Existence and molecular properties of a gas-phase, hydrogen-bonded complex between hydrogen fluoride and water established from microwave spectroscopy, J. Chem. Soc. Chem. Commun. . (1975) 341–343, http://dx.doi.org/10.1039/C39750000341.

[19] Z. Kisiel, A. Legon, D. Millen, Spectroscopic investigations of hydrogen bonding interactions in the gas phase. VII. The equilibrium conformation and out-of-plane bending potential energy function of the hydrogen-bonded heterodimer H_2O-HF determined from its microwave rotational spectrum, Proc. R. Soc. Lond. Ser. A Math. Phys. Eng. Sci. 381 (1982) 419, http://dx.doi.org/10.1098/rspa.1982.0081.

[20] Z. Kisiel, A. Legon, D. Millen, Potential constants for the hydrogen-bonded dimer H_2O...HF: Directional character of the hydrogen bond, J. Mol. Struct. 112 (1984) 1, http://dx.doi.org/10.1016/0022-2860(84)80237-9.

[21] A. Legon, D. Millen, Determination of properties of hydrogen-bonded dimers by rotational spectroscopy and a classification of dimer geometries, Faraday Discuss. Chem. Soc. 73 (1982) 71, http://dx.doi.org/10.1039/DC9827300071.

[22] J. Bevan, Z. Kisiel, A. Legon, D. Millen, S. Rogers, Spectroscopic investigations of hydrogen bonding interactions in the gas phase. IV. The heterodimer H_2O...HF: the observation and analysis of its microwave rotational spectrum and the determination of its molecular geometry and electric dipole moment, Proc. R. Soc. Lond. Ser. A Math. Phys. Eng. Sci. 372 (1980) 441–451, http://dx.doi.org/10.1098/rspa.1980.0121.

[23] G. Cazzoli, P.G. Favero, D.G. Lister, A.C. Legon, D.J. Millen, Z. Kisiel, The rotational spectrum of the hydrogen-bonded heterodimer H_2O...HF in the frequency range 40-80 GHz, Chem. Phys. Lett. 117 (1985) 543–546.

[24] S.P. Belov, V.M. Demkin, N.F. Zobov, E.N. Karyakin, A.F. Kupnov, I.N. Kozin, O.L. Polyansky, Tretyakov, M.Yu., Microwave study of submm spectra of H_2O...HF molecular complex, Preprint IPF AN SSSR. No. 192 (1988).

[25] Golubiatnikov G.Yu., S.P. Belov, I.I. Leonov, A.F. Andriyanov, I.I. Zinchenko, A.V. Lapinov, V.N. Markov, A.P. Shkaev, A. Guarnieri, Precision sub-Doppler millimeter and submillimeter lamb-dip spectrometer, Radiophys. Quantum El. 56 (2014) 599–609.

[26] N.F. Zobov, E.N. Karyakin, Investigation of submillimeter spectrum of the HF-dimer, Izv. VUZov. Radiofizika (in Russian) 31 (11) (1988) 1415–1417.

[27] S.P. Belov, E.N. Karyakin, I.N. Kozin, A.F. Krupnov, O.L. Polyansky, Tretyakov, M.Yu., N.F. Zobov, R.D. Suenram, W.J. Lafferty, Tunneling-rotation spectrum of the hydrogen fluoride dimer, J. Mol. Spectrosc. 141 (2) (1990) 204–222.

[28] H.M. Pickett, The fitting and prediction of vibration-rotation spectra with spin interactions, J. Mol. Spectrosc. 148 (1991) 371–377.

[29] S.E. Novick, A beginner's guide to Pickett's SPCAT / SPFIT, J. Mol. Spectrosc. 329 (2016) 1–7.

[30] B.J. Drouin, Practical uses of SPFIT, J. Mol. Spectrosc. 340 (2017) 1–15.

[31] M. Schafer, Weakly bound complexes: structure and internal motion data obtained from rotational spectra, J. Mol. Struct. 599 (2001) 57–67.

[32] Z. Kisiel, Tretyakov, M.Yu., O.L. Polyansky, Recovery of legacy paper spectra and new results on the rotational spectrum of H_2O...HF, in: The 64th Inter. Symp. Mol. Spectrosc., Columbus, Ohio, USA. June 22-26, 2009, Report FC04.

[33] R.K. Thomas, Hydrogen-bonding in vapor-phase between water and hydrogen-fluoride - infrared-spectrum of 1/1 complex, Proc. R. Soc. Lond. Ser. A Math. Phys. Sci. 344 (1975) 579.

[34] M. Quack, M.A. Suhm, Accurate quantum Monte Carlo calculations of the tunneling splitting in $(HF)_2$ on a six-dimensional potential hypersurface, Chem. Phys. Lett. 234 (1–3) (1995) 71–76.